Heat transfer in volcano–ice interactions on Mars: synthesis of environments and implications for processes and landforms

James W. HEAD, III,[1] Lionel WILSON[2]

[1]*Department of Geological Sciences, Brown University, Providence RI 02912 USA*
E-mail: james_head@brown.edu
[2]*Department of Environmental Science, Lancaster University, Lancaster LA1 4YQ, UK*

ABSTRACT. We review new advances in volcano–ice interactions on Mars and focus additional attention on (1) recent analyses of the mechanisms of penetration of the cryosphere by dikes and sills; (2) documentation of the glacial origin of huge fan-shaped deposits on the northwest margins of the Tharis Montes and evidence for abundant volcano–ice interactions during the later Amazonian period of volcanic edifice construction and (3) the circumpolar Hesperian-aged Dorsa Argentea Formation, interpreted as an ice sheet and displaying marginal features (channels, lakes and eskers) indicative of significant melting and interior features interpreted to be due to volcano–ice interactions (e.g. subglacial volcanic edifices, pits, basins, channels and eskers). In this context, we describe and analyse several stages and types of volcano–ice interactions: (1) magmatic interactions with ice-rich parts of the cryosphere; (2) subglacial volcanism represented by intrusion under and into the ice and formation of dikes and moberg-like ridges, intrusion of sills at the glacier–volcano substrate interface and their evolution into subglacial lava flows, formation of subglacial edifices, marginal melting and channels; (3) synglacial (ice contact) volcanism represented by flows banking up against glacier margins, chilling and forming remnant ridges and (4) post-glacial volcanism and interactions with ice deposits.

INTRODUCTION

As contributions to the first Volcano–Ice Interactions on Earth and Mars Conference in 2000 in Reykajvik, Iceland, we reviewed the basic principles of heat transfer and melting in subglacial basaltic volcanic eruptions and assessed the implications for volcanic deposit morphology and meltwater volumes (Wilson and Head, 2002). We also reviewed and synthesized the general environments and geological settings of magma–water interactions on Mars, applying our understanding of basic heat transfer mechanisms and citing and discussing numerous examples from different occurrences on Mars (Head and Wilson, 2002). We showed that a global cryosphere developed early in the history of Mars, and that water and related volatiles were sequestered within and below this global cryosphere, interacting with magmatism (plutonism and volcanism) throughout the history of Mars. We outlined theory and observations for magma–water interactions to have formed massive pyroclastic deposits, large-scale ground collapse and chaotic terrain, major outflow channels, mega-lahars, subpolar ice sheet eruptions and subglacial edifices, pseudocraters and hydrothermal sites.

In subsequent years, numerous developments have been made in the study of volcano–ice interactions on Mars, and in the theory of volcano–ice interactions on Earth and Mars. For example, analytical thermal models have recently been used to reassess the efficiency with which heat can be transferred from magma to ice in three situations: lava flows erupted on top of glacial ice, sill intrusions beneath glacial ice evolving into subglacial lava flows and dike intrusions into the interiors of glaciers (Wilson and Head, 2007). In this contribution, we highlight advances in the last five years in the understanding of the distribution of ice on the surface of Mars and in the Martian cryosphere, and provide new insights into the importance of volcano–ice interactions.

In our previous review and synthesis of the general environments and geological settings of magma–H_2O interactions on Mars (Head and Wilson, 2002) we described the global cryosphere that developed early in the history of Mars (Clifford, 1993) as well as the ice, groundwater and related volatiles sequestered within and below this global cryosphere. Figure 1 depicts the transition from a vertically integrated hydrologic system and cycle to a horizontally structured (layered) hydrologic system in which the cryosphere serves to minimize contact between the surface and the groundwater system below. In the Noachian and Early Hesperian (Fig. 1a) enhanced heat flux caused bottom-up heating and a 'warm, wet' early Mars atmosphere scenario would have provided top-down heating. Together these would have resulted in no cryosphere in the equatorial and mid-latitude regions. Pluvial activity caused runoff and soaked into the regolith, recharging the groundwater system. The hydrological system was thus vertically integrated.

Magmatism (plutonism and volcanism) has interacted with this hydrologic system throughout the history of Mars (Carr, 1996). By the Amazonian period, the cryosphere was generally globally continuous and the major surface and near-surface ice reservoirs were the regolith (particularly at higher latitudes), the shallow part of the underlying megaregolith and the polar ice deposits (Fig. 1). Variations in orbital parameters led to significant migration and exchange between these reservoirs during the Amazonian. For example, during periods of high obliquity, sublimated polar ice was transported in the atmosphere (e.g. Forget and others, 2006) and deposited at mid to high latitudes to form a mantle (e.g. Head and others, 2003a). In mid-latitudes, lobate debris aprons and lineated valley fill were formed (e.g. Neukum and others, 2004; Head and others, 2003a, 2005b, 2006a, b), and in equatorial regions huge tropical mountain glaciers were formed (e.g. Head and

https://doi.org/10.3189/172756407782282570 Published online by Cambridge University Press

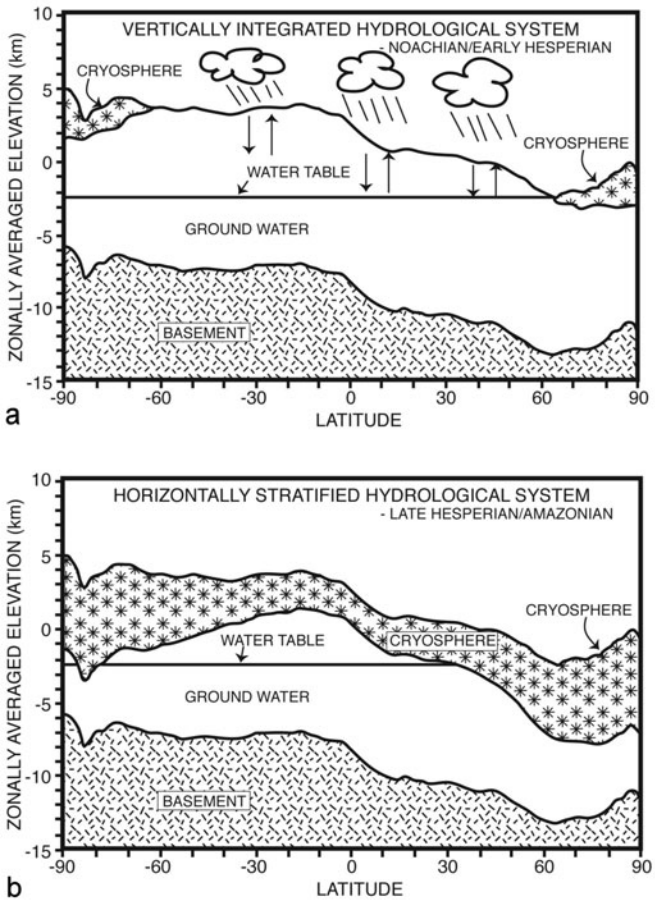


Fig. 1. The transition from a vertically integrated hydrologic system and cycle to a horizontally structured (layered) hydrologic system: (a) during the Noachian and Early Hesperian, enhanced heat flux caused bottom-up heating and a 'warm, wet' early Mars atmosphere scenario would have provided top-down heating and (b) in the Late Hesperian through the Amazonian up to the present, bottom-up and top-down heating both decreased and a global cryosphere developed, sequestering the groundwater into the subsurface and forming a horizontally stratified hydrologic system.

Marchant, 2003; Shean and others, 2005). These two scenarios provide the evolving framework for volcano–ice interactions on Mars (Head, 2006). Current cryosphere thickness estimates and depth to basement are derived from Clifford (1993).

In our earlier contributions (Wilson and Head, 2002; Head and Wilson, 2002), we outlined theory and observations for magma–water interactions to have formed (1) massive pyroclastic deposits; (2) large-scale ground collapse and chaotic terrain (due to sills); (3) major outflow channels (due to dikes); (4) mega-lahars dwarfing terrestrial examples; (5) subpolar ice sheet eruptions and edifices; (6) pseudocraters; (7) landslides on volcanic edifice flanks and (8) hydrothermal sites. In this analysis, we review recent advances in these areas and focus additional attention on newly documented dike–sill interactions with the cryosphere, tropical mountain glaciers at the Tharsis Montes and Olympus Mons, and the south circumpolar Dorsa Argentea Formation, interpreted to be an ice sheet. We assess these new developments in terms of magma–cryosphere interactions and surface ice deposit–magma interaction in synglacial and post-glacial circumstances.

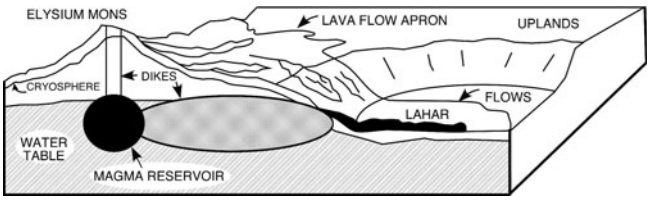


Fig. 2. The Elysium Rise, showing the locations of dike emplacement events causing outflow of sequestered groundwater in the form of aqueous floods and lahars. Dikes reaching the surface above the water table led to effusive eruptions. On the other side of the rise, radial dikes cracked the cryosphere at Cerberus Rupes and released groundwater and lava (e.g. Head and others, 2003b).

NEW PERSPECTIVES ON VOLCANO–ICE INTERACTIONS

Magmatic interactions with ice-rich parts of the global cryosphere

The formation of the huge outflow channels (e.g. Baker, 2001) has historically been related to the catastrophic release of groundwater from beneath a cryospheric seal, either by melting of ground ice, or cracking of the cryosphere and catastrophic release of groundwater held under hydrostatic pressure. Recent work has shown evidence that the release events were not simply related to tectonic faulting, but rather were linked to dike emplacement events that not only crack the cryosphere, but provide sufficient melting adjacent to the dike so that significant water outflow can occur. For example, on the southeast flanks of Elysium, in the Cerberus region of Elysium Planitia (Fig. 2), geologic observations provide evidence for combined events including dike emplacement, lava extrusion and massive outflow of water (e.g. Head and others, 2003b). Geological observations suggest that predicted aqueous fluxes can be accommodated by flow through a dike-related cryospheric fracture ~2 m wide. The models also show that little melting of the cryosphere occurs due to the dike emplacement event and that the vast majority of the flow is due to released groundwater.

On the western flanks of Elysium, dike emplacement events are thought to have led to two types of eruptions (e.g. Russell and Head, 2003). Dikes intruded to near-surface depths low on the western flanks of Elysium apparently cracked the cryosphere below the groundwater table, leading to the release of groundwater, volcanic ash and debris, and the emplacement of a series of mega-lahars, extending hundreds of kilometers out into the Utopia Basin. Higher on the flanks of Elysium, presumably above the water table, dike-fed eruptions produced only lava flows and pyroclastics (Fig. 2). Furthermore, in a nearby location at the head of Hrad Valles, dike emplacement apparently led to shallow sill formation producing a near-surface phreatomagmatic eruption related to violent mechanical and thermal mixing between the sill and the ice-rich substrate overlying the groundwater zone (e.g. Wilson and Mouginis-Mark, 2003).

In the circum-Tharsis region, where most of the outflow channel sources occur (Carr, 1996), detailed analysis of the Mangala Valles source region shows that dikes radiating from the central part of Tharsis (e.g. Wilson and Head, 2002) are likely to be the cause of the outflow event there. The source of Mangala is within a graben radial to Tharsis (e.g. Ghatan and others, 2005) and the source region is characterized by a series of parallel dune-like ridges extending in

https://doi.org/10.3189/172756407782282570 Published online by Cambridge University Press

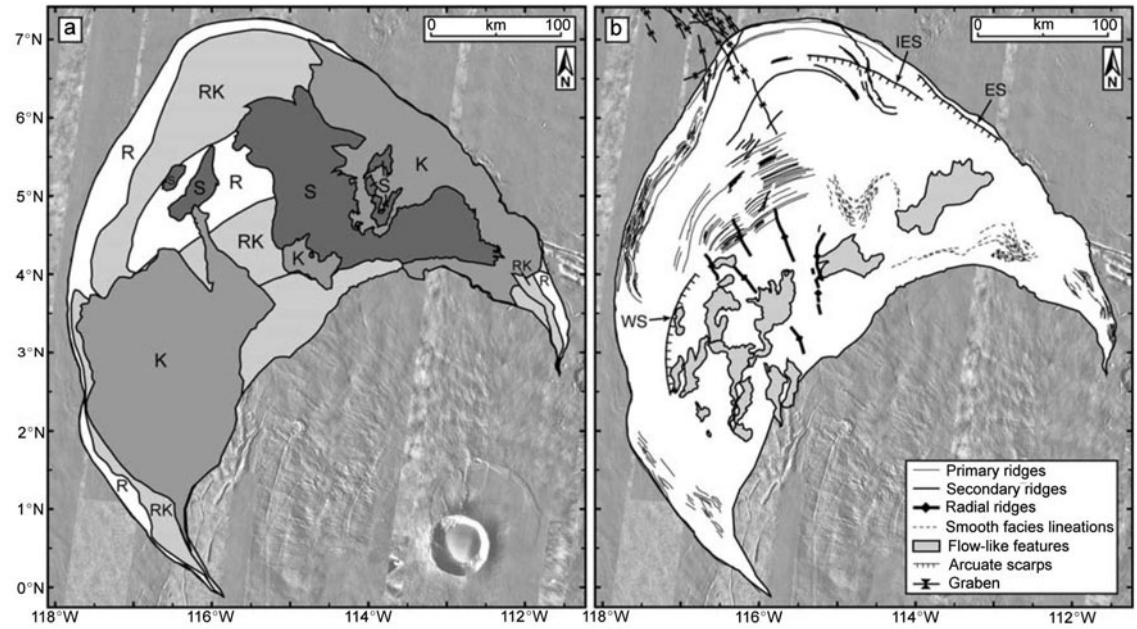


Fig. 3. (a) Sketch map showing the main features and facies of the fan-shaped deposit, interpreted to be the remnant of a cold-based glacier: R (ridged); K (knobby); S (smooth); RK (transitional);. (b) Sketch map of flow-like features and ridges interpreted to be subglacial and englacial deposits: ES (eastern scarp); IES (inner eastern scarp); WS (western scarp) (after Shean and others, 2005).

a band for up to 25–30 km around the eastern margin of the source (e.g. Wilson and Head, 2004). These ridges are interpreted to have formed during initial phreatomagmatic activity caused by dike emplacement, cryospheric cracking, mixing of magma and groundwater and explosive eruption to the surface. Fragmented magma, steam and country rock erupted to the surface and expanded from a choked state at the vent to form a near ballistic, Io-like eruption plume, forming the dunes by outward high-velocity flow of the plume (Wilson and Head, 2004). This initial stage was immediately followed by the outpouring of groundwater and carving of the Mangala channel system (e.g. Ghatan and others, 2005); evidence of glacial deposits on the rim supports the interpretation that the climate then was similar to current Mars conditions (e.g. Head and others, 2004). Thus, a variety of studies continue to underline the importance of dike emplacement in the cracking of the cryosphere and the release of groundwater.

Sills intruded into an ice-rich cryosphere have also been shown to be effective sources of melting due to their more efficient heat transfer to ice-rich material than dikes (e.g. Head and Wilson, 2002). Contact of magma and ice-rich substrate in dikes is limited by the thickness of the cryosphere, whereas sills extend laterally into the ice-rich substrate and expand in thickness, optimizing the transfer of heat to ice-rich material and potential melting. In the Tharsis region, Leask and others (2006a) have presented the case that Aromatum Chaos, the source depression at the head of the Ravi Valles outflow channel (Leask and others, 2006b), was the site of a sill intrusion, causing heating, melting, groundwater release and outflow. Specifically, they use the vertical extents and displacements of terrain blocks associated with the depression floor, and estimates of cryospheric thickness, to constrain the vertical extent of ice melting and the thickness of the sill. The intrusion of a shallow sill was very efficient in breaching the cryospheric seal above the pressurized water table. They show that at least ~75% of the volume removed from the Aromatum depression was crustal rock rather than melted ice, and that water from the melted cryosphere played a minimal role in formation of both the depression and the outflow channel itself.

Subglacial volcanism represented by intrusion into the ice and the formation of dikes and moberg-like ridges

Wilson and Head (2002) outlined the theoretical basis for the emplacement of dikes into glacial ice and the formation of sills at the glacier-country rock contact (the base of the glacier). Magma emplacement velocity and strain rate associated with dike and sill intrusion events are high, and these processes occur much faster than heat can be transferred into the ice to cause melting. Thus, in the initial stages of dike and sill emplacement events, glacial ice behaves as a rock; Wilson and Head (2002) presented theoretical analyses suggesting that these types of events should occur on Earth. Analysis of new Mars data reveals evidence for dike emplacement events in several different apparently ice-rich environments. Head and others (2006c) have recently described dikes of Hesperian age that have been exhumed from below a regional mantle that is thought to have been ice-rich. Recent studies have documented the presence of fan-shaped deposits representing tropical mountain glaciers on the northwest flanks of the Tharsis Montes (e.g. Head and Marchant, 2003; Shean and others, 2005) and Olympus Mons (e.g. Milkovich and others, 2006). At Pavonis and Arsia Mons, ice sheets are likely to have exceeded 2 km in thickness (e.g. Fastook and others, 2005) and glaciation clearly took place contemporaneously with volcanism, with evidence of pre-glacial, synglacial and post-glacial magma intrusion and extrusion.

Detailed examination of these deposits reveals evidence for dike emplacement into the glacier and subglacial sill/flow

https://doi.org/10.3189/172756407782282570 Published online by Cambridge University Press

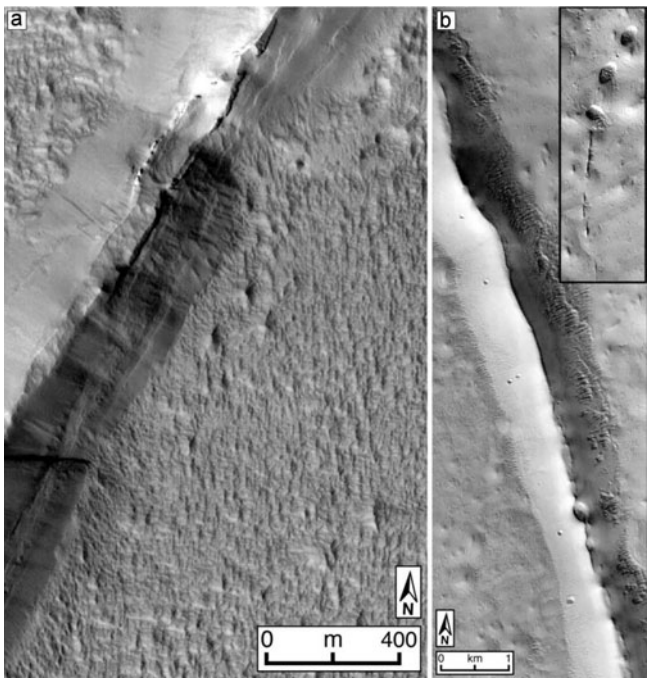


Fig. 4. Mars Orbiter Camera (MOC) images showing details of the ridges interpreted to be remnants of dikes intruded into the former glaciers. (a) Narrow ridge with sharp-ridge crest; peak is split and very sharp along the ridge crest. (b) Narrow ridge with sharp ridge crest; inset is ~15 km NNW and shows pits and en echelon-like ridge structure. Illumination from the left in all cases (after Shean and others, 2005).

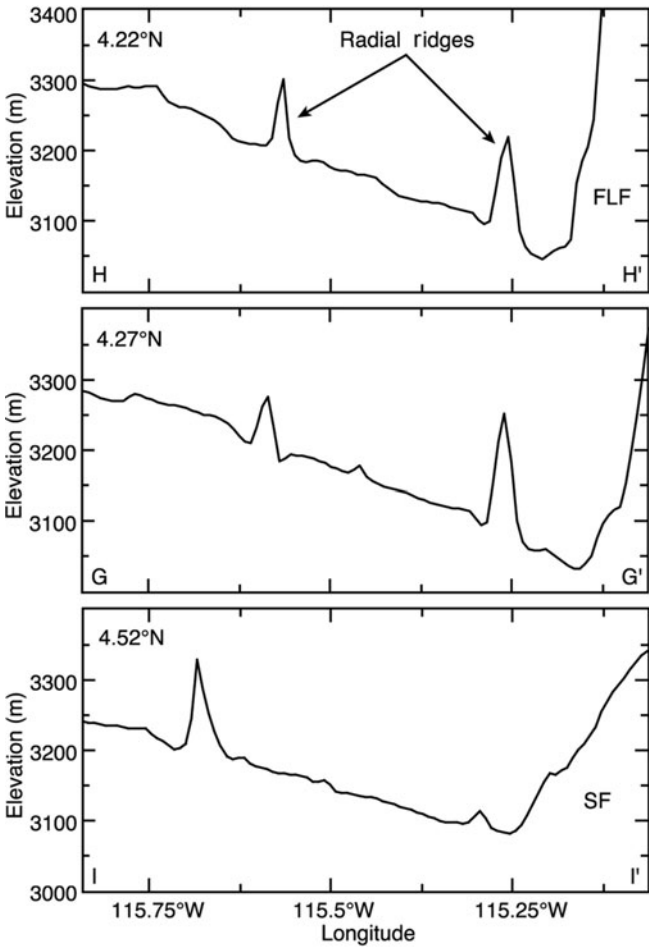


Fig. 5. MOLA altimetric profiles showing the height and width of the ridges interpreted to be dike remnants (see images in Fig. 4). Lines of sections are shown in Fig. 6a. FLF (flow-like features); SF (smooth facies) (after Shean and others, 2005).

emplacement. For example, radial ridges within the Pavonis Mons fan-shaped deposits display unique morphologies similar to those of eroded and exposed terrestrial dikes and transition to the kinds of shallow graben typical of near-surface dike intrusion outside the deposit (Shean and others, 2005) (Figs 3–10). High-resolution images of these radial ridges (Fig. 4) reveal symmetric ridges of debris capped by narrow linear outcrops along the ridge crest. Altimetry data show that the radial ridges typically rise more than 150 m above the surrounding terrain (Fig. 5). Using the mean heights and widths of the exposed ridges, Wilson and others (2005) reconstructed mean dike widths of ~20 m and showed that these values were consistent with plausible reservoir geometries for radial dike emplacement events from a magma reservoir below the Pavonis Mons volcano summit.

Chapman (1994) and Chapman and others (2000) described ridges in Utopia Planitia that they interpreted to have formed during eruptions beneath an ice sheet (frozen paleolake?), forming hyaloclastite ridges. Head and Wilson (2002) examined these features with new Mars Orbiter Laser Altimeter (MOLA) data and showed that they were ~100–200 m in height with evidence for central summit depressions, consistent with production by volcano–ice interaction and subsequent modification (flooding and embayment) by later flow events. New Thermal Emission Imaging System (THEMIS) data for these features (Figs 11–12) further illustrate their unusual texture and structure. In the newer high-resolution data, individual summit pits can be seen along the crest of the moberg-like ridge (Fig. 11) and in the broader structure, dike-like features can be seen emanating from its base in both directions along strike (Fig. 12).

Subglacial volcanism represented by the intrusion of sills at the glacier–volcano substrate interface and their evolution into subglacial lava flows

Wilson and Head (2002) showed that magma initially intruded laterally at the basal ice–substrate contact and spread sideways as a sill. Marginal chilling and continued intrusion can lead to preferential upward growth of the sill (inflation). Confining pressure of the overlying ice and meltwater can inhibit vesiculation. When adjacent and overlying meltwater drains and contact with the atmosphere is established, the pressure decreases dramatically and explosive eruptions can ensue. As the subglacial sill emplacement event effectively becomes subaerial, the magma body becomes thicker, narrower and flows faster, changing from a sill to a thick lava flow-like structure.

In addition to radial ridges, the Pavonis Mons fan-shaped deposits (Figs 3–10) also display anomalous steep-sided lobate flow-like features (Fig. 6) that are interpreted to be subglacial lava flows (e.g. Shean and others, 2005). These features occur within the fan-shaped deposits, are generally covered by glacial facies and occur in close association with the radial ridges interpreted to be dikes (compare Figs 3 and 6). Flow-like features emerge from vent-like structures, and extend for several tens of kilometers. One of the dike-like radial ridges expands into a pancake-like feature that is interpreted to represent a subglacial sill. The individual

https://doi.org/10.3189/172756407782282570 Published online by Cambridge University Press

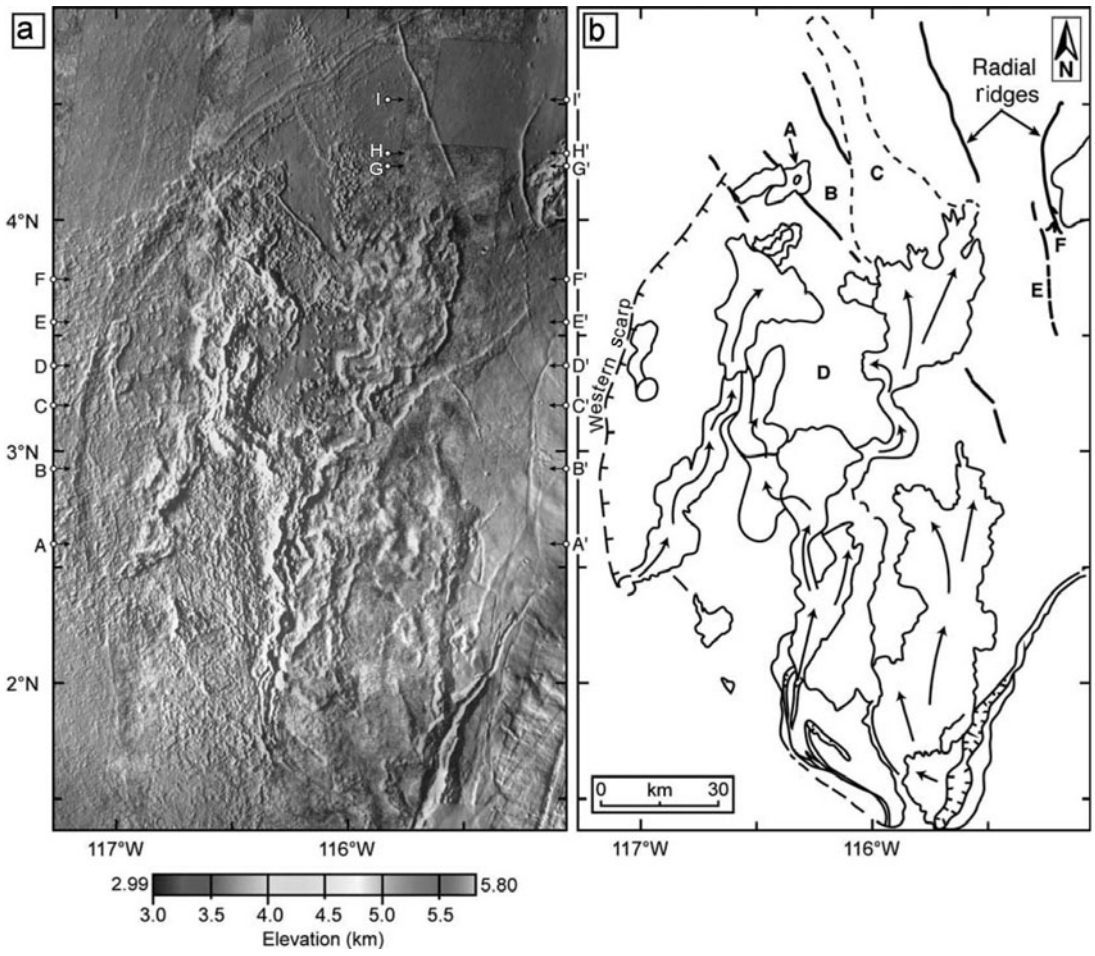


Fig. 6. Steep-sided flow-like features (FLF) occurring beneath the fan-shaped deposits and interpreted to be emplaced as subglacial sills and flows. (a) Image mosaic of the areas. Letters at margins indicate profile locations (Figs 5 and 7). (b) Sketch map showing steep-sided features, ridges and interpreted direction of flows (arrows). A (subglacial sill); B (few knobs or hills); C (dense concentration of knobby ridges); D (knobby facies sparse or absent); E (en echelon ridge); F (forked ridge) (after Shean and others, 2005).

lobate flow-like features have very steep sides, and are up to several hundred meters thick (Fig. 7), many times thicker than typical adjacent subaerial flanking flows on the edifice, and unlike flows of any other composition yet observed on Mars. These thick flow-like features also have raised levee-like ridges on their margins (Figs 6 and 7), suggestive of flow margin buildup and subsequent central flow advance or flow center collapse due to degassing.

Subglacial volcanism represented by the formation of edifices

The set of Hesperian-aged south circumpolar deposits represented by the Dorsa Argentea Formation (e.g. Tanaka and Scott, 1987; Tanaka and Kolb, 2001; Head and Pratt, 2001) has been interpreted to be a volatile-rich polar deposit representing more than twice the area of the present Amazonian-aged layered terrain and residual polar ice, which it currently underlies. This huge polar ice-related deposit makes up about 2% of the surface of Mars and has undergone significant evolution since its emplacement. Evidence for melting and drainage within the deposits includes large kilometer-scale pits and troughs, esker-like ridges within and at the margins, a large lake basin at one edge and sinuous channels that lead away from the edge, extending for hundreds of kilometers into surrounding lows such as the Argyre basin (e.g. Head and Pratt, 2001). Although the relative roles of sources of melting (e.g. top-down: atmospheric evolution and insolation changes and/or bottom-up: geothermal gradient, intrusion and extrusion) are debated, the deposits preserve ample evidence for ice–volcanism interaction.

Particularly striking are candidate subglacial volcanoes within the deposit. Ghatan and Head (2002) described 17 anomalous mountains (originally mapped by Tanaka and Scott (1987) and now called Sisyphi Montes) that form an unusual cluster in the central part of the Dorsa Argentea Formation. The mountains occur over a large area (Fig. 13), have separation distances of ~175 km, are typically 30–40 km in diameter, ~1000–1500 m high, with their bases near ~1200 m elevation. Many members of this population are located on or adjacent to a 660 km long line extending toward the south pole (Figs 13–15). On the basis of their morphology, distinctiveness, alignment and isolation relative to other landforms, these features have been interpreted to be predominantly of volcanic origin (Ghatan and Head, 2002). A significant number of these features are unusually shaped, such as flat-topped, with or without summit cones, or have large summit craters relative to summit diameter. Several of the mountains display sinuous channels around their margins and bases. Ghatan and Head (2002) interpreted these and other characteristics to mean that many of the mountains represented volcanoes that had erupted

https://doi.org/10.3189/172756407782282570 Published online by Cambridge University Press

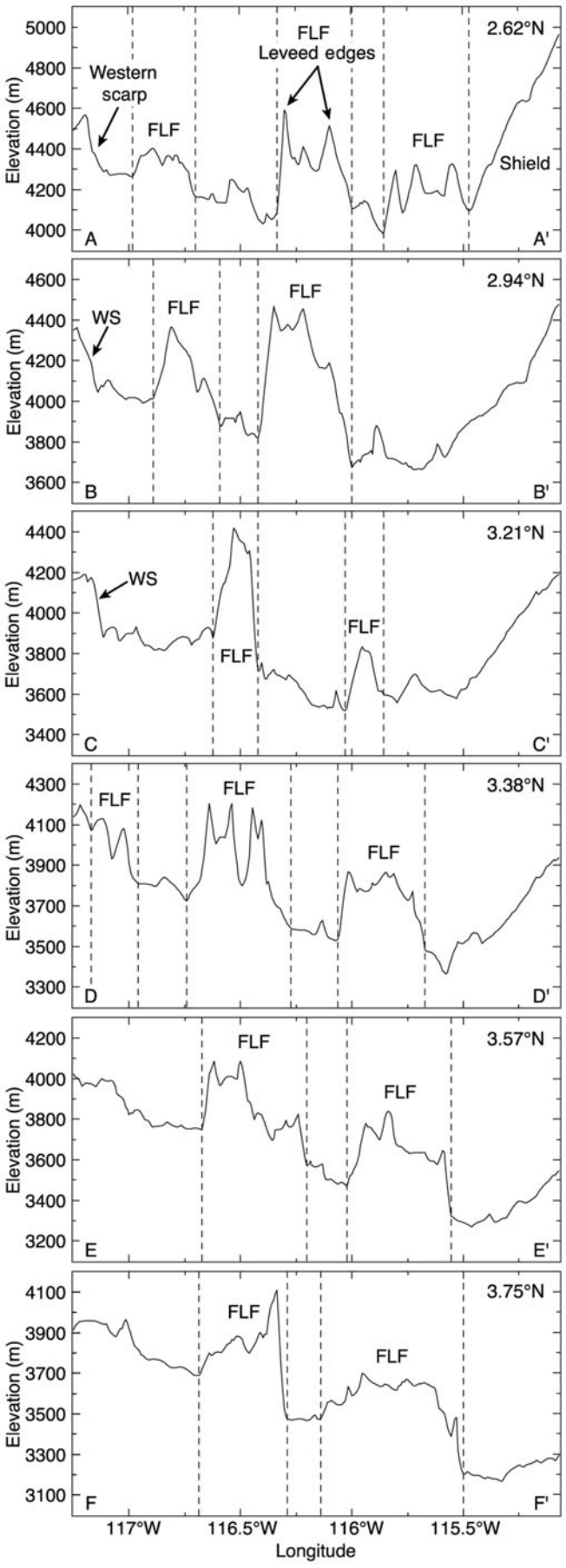


Fig. 7. MOLA altimetric profiles showing the steep sides and levees characteristic of the flow-like features (FLF) interpreted to have been intruded below the fan-shaped glacier. Locations of profiles shown in Figure 6 (after Shean and others, 2005).



Fig. 8. THEMIS image showing broad occurrence of channels apparently emerging from beneath cold-based glacial deposits (bottom of image) and interpreted to represent meltwater outflow following subglacial volcano–ice interaction and melting (after Shean and others, 2005).

subglacially beneath the Dorsa Argentea Formation (tuya-like features) and that the meltwater products could be traced from these regions to the margins of the deposit where they drained along eskers and channels into adjacent lakes or distant basins. The topography of the mountains suggested that the ice sheet averaged at least 1.4 km thick at the time of the eruptions.

Elsewhere in the Dorsa Argentea Formation, the topography is disrupted by a series of large irregular depressions (Cavi Angusti; Fig. 16) whose origin has been attributed to eolian deflation and subglacial melting (e.g. Ghatan and others, 2003). Analysis of the largest of these depressions (~50–100 km in diameter and up to about 1500 m deep; Fig. 17) shows terraced interiors, centrally located equidimensional and elongated structures interpreted to be edifices, and associated lava flow-like structures. The equidimensional mountain is ~12 km in diameter and ~770 m high, is centrally located within the basin, has anomalously steep sides and a flat top. It is perched on a low platform with lobate edges, extending about 2.5 km away from the edifice base in all directions. A lobate flow-like feature, 30 km long and 14 km wide with clear terminal scarps, extends away from the base of the mountain towards the north, parallel to the elongate trend of the basin. The elongated structure is a ridge located to the northwest of the central mountain, oriented in the direction of the long axis of the basin, has a similar height and also rests on a platform. Together, these edifices and lobate structures are interpreted to be volcanic edifices and associated lava flows. Their central location in the depression in the Dorsa Argentea Formation (Figs 16 and 17) strongly suggests that these

https://doi.org/10.3189/172756407782282570 Published online by Cambridge University Press

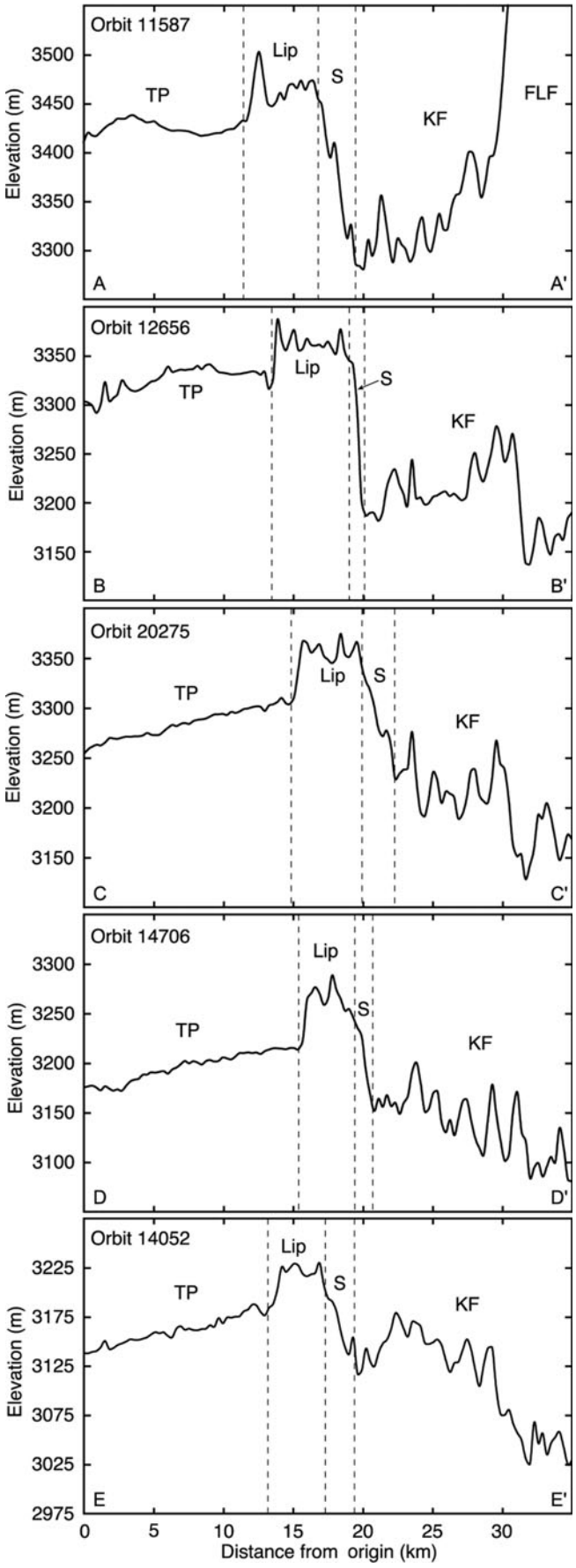


Fig. 9. MOLA altimetric profiles of the steep-sided ridge at the margin of the depression containing the majority of the cold-based glacial deposits at Pavonis Mons (see also Fig. 3). TP (Tharsis plains); S (scarp); KF (knobby facies) (after Shean and others, 2005).

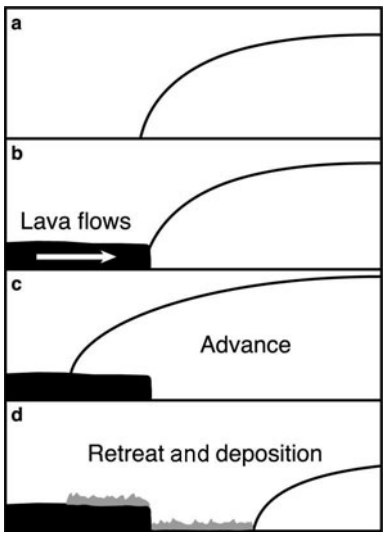


Fig. 10. Sketch showing the interpreted sequence of events in the formation of the ridge by the encounter and interaction of lava flows with the glacier. Grey represents glacial deposits left by the later advance and retreat of the glacier (after Shean and others, 2005).

features represent subglacial eruptions, and that their formation is directly related to the presence of the large depression interpreted to be due to volcano–ice interactions and melting (e.g. Ghatan and others, 2003). Volume estimates and heat transfer calculations by Ghatan and others (2003) are consistent with such a mechanism involving a combination of intrusion and subglacial extrusion similar to that observed in Icelandic subglacial eruptions and meltwater generation (e.g. Guðmundsson and others, 1997).

Image resolution is currently insufficient to determine detailed microenvironments predicted from observed terrestrial eruptions and deposits and theoretical considerations (e.g. Wilson and Head, 2002). We speculate, however, that the platforms at the base of the edifices may be sills initially formed at the ice sheet–substrate interface, and that they then evolved in subsequent stages as subglacial edifices and ultimately subaerial eruptions as the ice cover melted and drained. Furthermore, regional topography and ice-sheet geometry strongly suggest that any meltwater generated would drain to the north into the adjacent low areas. Evidence that this occurred includes an outlet and broad sinuous channel at the northern end of the largest depression (Fig. 17), an unusual set of features interpreted to be a lake margin environment (e.g. Dickson and Head, 2006) at the edge of the Dorsa Argentea Formation less than ~150 km to the north of the basin and a 300–800 km depression interpreted to be the site of a lake, which itself drains to the north into the Argyre basin (Head and Pratt, 2001). Seven additional basins in Cavi Angusti contain mountains and ridges, usually centrally located, which are also interpreted to represent the remnants of subglacial eruptions, formation of englacial lakes, and subsequent meltwater drainage to the north (Ghatan and others, 2003). In summary, new spacecraft data support the interpretation that a significant part of the geomorphology of the Cavi Angusti region of the Dorsa Argentea Formation is plausibly interpreted to be due to volcano–ice interactions (Ghatan and others, 2003), an interpretation originally proposed by Howard (1981) using low-resolution image data.

https://doi.org/10.3189/172756407782282570 Published online by Cambridge University Press

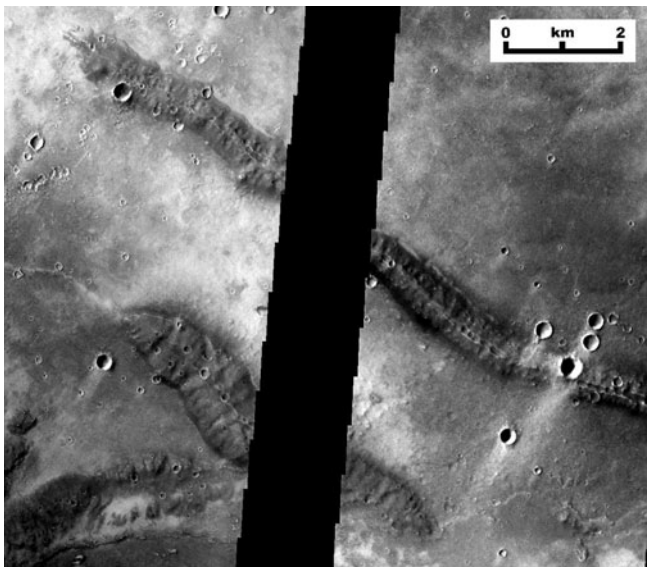


Fig. 11. New Mars Odyssey THEMIS images revealing details of the structure and morphology of ridges and hills in the western Elysium/eastern Utopia region of Mars, interpreted to be analogous to moberg ridges on Earth (see Chapman, 1994; Chapman and others, 2000; Head and Wilson, 2002, fig. 16).

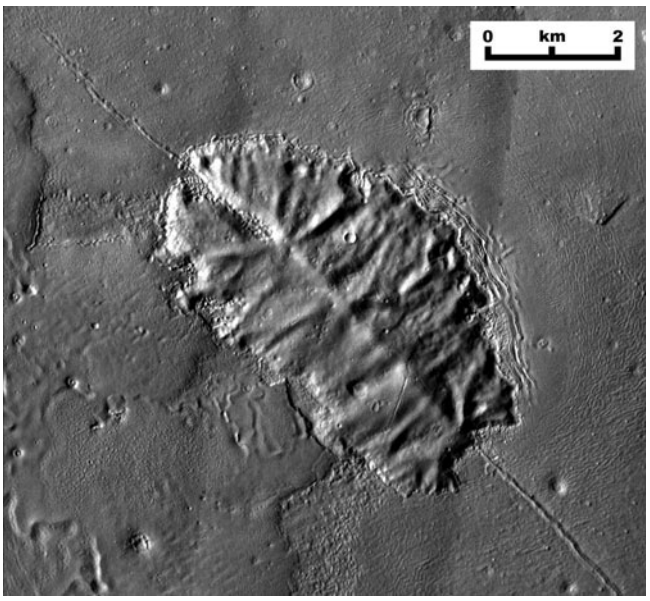


Fig. 12. New Mars Odyssey THEMIS images revealing details of the structure and morphology of ridges and hills in the western Elysium/eastern Utopia region of Mars interpreted to be analogous to moberg ridges on Earth (see Chapman, 1994; Chapman and others, 2000; Head and Wilson, 2002, fig. 16). The linear ridge extending from each side of the complex mound is interpreted to be the surface manifestation of a dike; eruptions continued in the central part of the structure along the strike of the dike, building a complex moberg-like ridge.

Subglacial volcanism represented by marginal melting and channels

The cold, hyperarid Martian environment typical of the greater part of the history of Mars is conducive to the formation of cold-based glaciers as opposed to wet-based glaciers (e.g. Head and Marchant, 2003; Marchant and Head, 2003). Cold-based glaciers involve little to no meltwater generation unless they become thick enough to become polythermal (wet-based in the interior and cold-based at the margins), or volcano–ice interactions generate meltwater at the base or within the glacier. Thus, the presence of marginal eskers, channels, lakes or other evidence of meltwater and drainage provides hints of the former presence of subglacial melting due to either polythermal ice conditons or volcano–ice interactions. Such features are seen in several places on Mars.

The margins of the huge south circumpolar Dorsa Argentea Formation (Fig. 13), interpreted to be a Hesperian-aged polar ice sheet (e.g. Head and Pratt, 2001), show evidence of extensive eskers (e.g. Head and Hallet, 2001; Head and Pratt, 2001), marginal lakes (e.g. Milkovich and others, 2002; Dickson and Head, 2006) and drainage channels extending from the Dorsa Argentea Formation margins for hundreds of kilometers into surrounding depressions such as the Argyre basin (Milkovich and others, 2002; Head and Pratt, 2001; Ghatan and Head, 2004). Although polythermal ice conditions (due to the accumulation of polar ice deposits to thicknesses in excess of 3–4 km, thus raising the melting geotherm into the base of the thickest part of the ice permitting basal melting) or higher global geothermal gradients in earlier Martian history cannot be ruled out, evidence that a significant part of the meltwater is related to subglacial volcano–ice interactions is compelling. For example, the eastern part of the volatile-rich Dorsa Argentea Formation shows evidence of meltback, drainage and ponding of meltwater (Milkovich and others, 2002) adjacent to the region of interpreted subglacial volcanoes (e.g. Ghatan and Head, 2002) (Fig. 13). Channels leading from the margins of the Dorsa Argentea Formation (Figs 18 and 19) enter nearby craters, and channels connecting the craters provide evidence for extensive crater flooding, ponding and filling, overtopping and downcutting. Further drainage occurs through a series of craters into the Prometheus Basin, over a distance of ~600 km and involving a total vertical drop of ~800 m. Topographic evidence (entry and exit elevations) indicates that water filled some craters to depths of at least 200 m and possibly up to 600 m with a minimum volume of 10^{12} m^3.

Along the central and western margins of the Dorsa Argentea Formation (Fig. 13), five sinuous valleys begin near the Dorsa Argentea Formation edge and are carved into surrounding Noachian cratered terrain, extending for distances of up to 1600 km before emptying into the Argyre Basin, ~1–3 km below their starting elevations (Head and Pratt, 2001; Ghatan and Head, 2004) (Fig. 20). The extension of these valleys into the Dorsa Argentea Formation can be traced for hundreds of kilometers due to the presence of aligned linear pits and basins and some preserved esker-like features on their floors (Ghatan and Head, 2004). The directions lead to the regions of Sisyphi Montes, the collection of isolated and aligned mountain features interpreted to be subglacial volcanoes (Figs 13–15; Ghatan and Head, 2002). These examples provide criteria to help locate subglacial melting environments and to test for links to distinguish between basal melting due to ice sheet thickening and volcano–ice interactions.

Minor examples of possible meltwater generation exist along the margins of Tharsis Montes tropical mountain glacial deposits. For example, at Pavonis Mons, candidate fluvial features occur locally at the northeast margin (Fig. 8)

https://doi.org/10.3189/172756407782282570 Published online by Cambridge University Press

of the cold-based glacial deposit (e.g. Shean and others, 2005). Here, the features form a broad 10–20 km wide set of channels that appear to emerge from beneath the deposit (bottom of Fig. 8) and extend downslope. These are interpreted to be local examples of meltwater discharge generated from melting associated with the dike/sill/lava flow ice–volcano interactions beneath the cold-based ice sheet. In contrast to the individual meltwater drainage channels seen surrounding the margins of the south circumpolar Dorsa Argentea Formation, these may be candidates for broader discharges similar to the jökulhlaups emerging from beneath Icelandic glaciers following subglacial eruptions (e.g. Björnsson, 1992).

Synglacial volcanism represented by flows banking up against glacier margins, chilling and forming remnant ridges

The presence of regional glaciers can also influence the nature of contemporaneous volcanic activity and deposits due to marginal interactions. For example, in the Tharsis Montes, volcanic and glacial activity appear to have been contemporaneous over periods of tens to hundreds of millions of years, and numerous lava flows emerging from volcano flank vents appear to have flowed along the margins of the tropical mountain glaciers, chilled, and built anomalously thickened lava flow deposits that are preserved today as asymmetric scarps following the removal of the glacial ice. For example, a significant ridge and scarp are observed along the northeast margin of the Pavonis tropical mountain glacier deposit (e.g. Shean and others, 2005) (Fig. 3). The current glacial deposits lie at elevations of up to 200 m below the level of the adjacent Tharsis volcanic plains (Fig. 9). The location of the ridge, its asymmetrical nature and the low elevation of the remnant deposits below the surrounding plains are all consistent with the interaction between lava flow and glacier margin. In this scenario (Fig. 10), lava flows emerged from the upper flanks of Pavonis, flowed downslope, encountered the flanking glacier, flowed around the margin for about 80 km, chilling and building a ridge before diverging from the front of the glacier

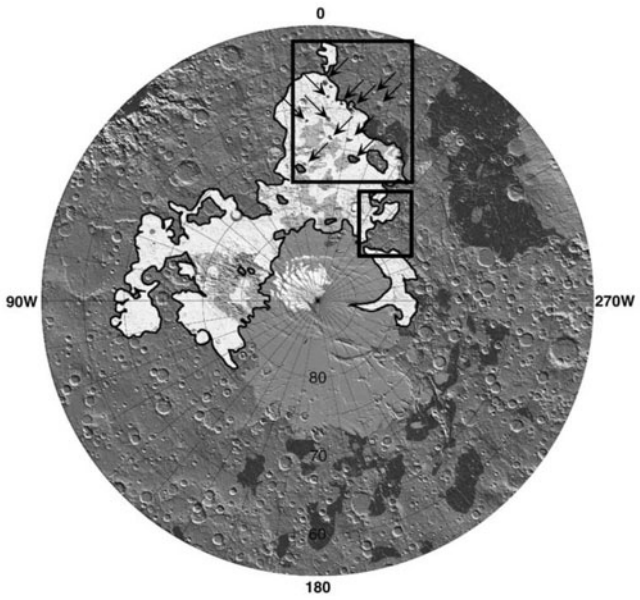


Fig. 13. Generalized geological map of the south polar region showing the distribution of the current polar deposits (white and dark gray around the pole), the Dorsa Argentea Formation (white and light gray in the upper left), and Hesperian ridged plains (black). Background is largely Noachian-aged cratered terrain. Large box shows location (arrows) of many of the mountains (Sisyphi Montes) interpreted to be subglacial eruptions (Ghatan and Head, 2002) (Figs 14 and 15), and the small box shows the location of marginal meltwater channels thought to be drainage routes for volcano–ice interaction melting products (Figs 18 and 19) (Milkovich and others, 2002).

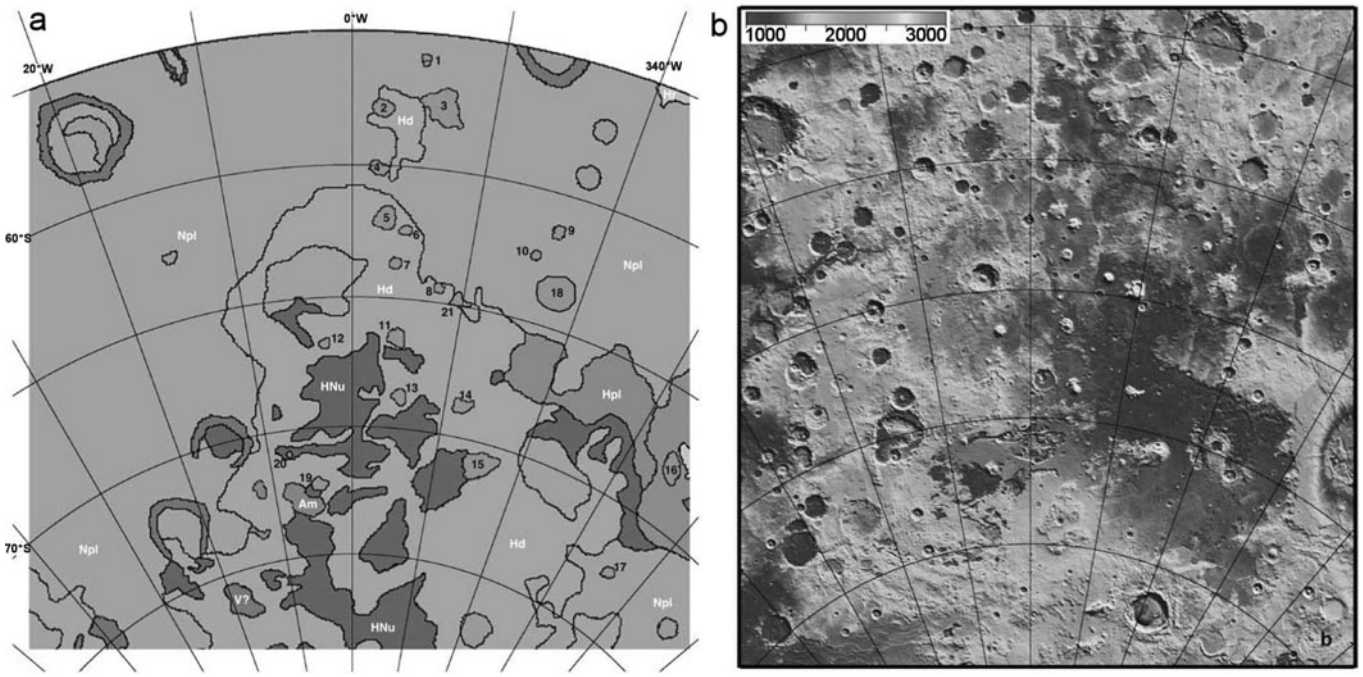


Fig. 14. Enlargement of the location of the mountains interpreted to be subglacial volcanoes (Fig. 13) (Ghatan and Head, 2002). (a) Sketch map: Npl (Noachian heavily cratered terrain); HNu (undivided terrain); Hd (Dorsa Argentea Formation). Numbers refer to individual edifices. (b) MOLA altimetry map.

https://doi.org/10.3189/172756407782282570 Published online by Cambridge University Press

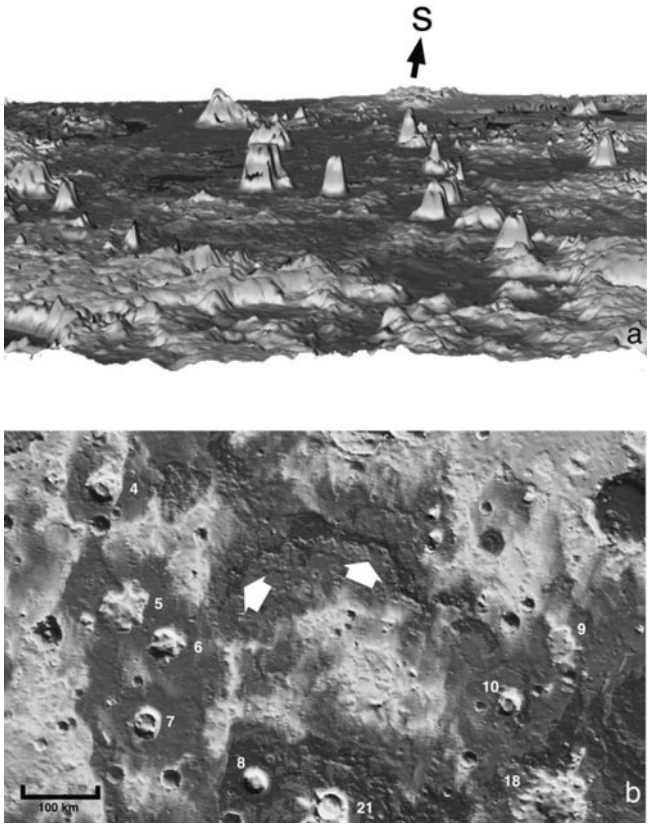


Fig. 15. Perspective (a) and vertical views (b) of the main cluster of interpreted subglacial volcanoes intruded beneath the Dorsa Argentea Formation ice sheet. Note the channel indicated by arrows (Ghatan and Head, 2002).

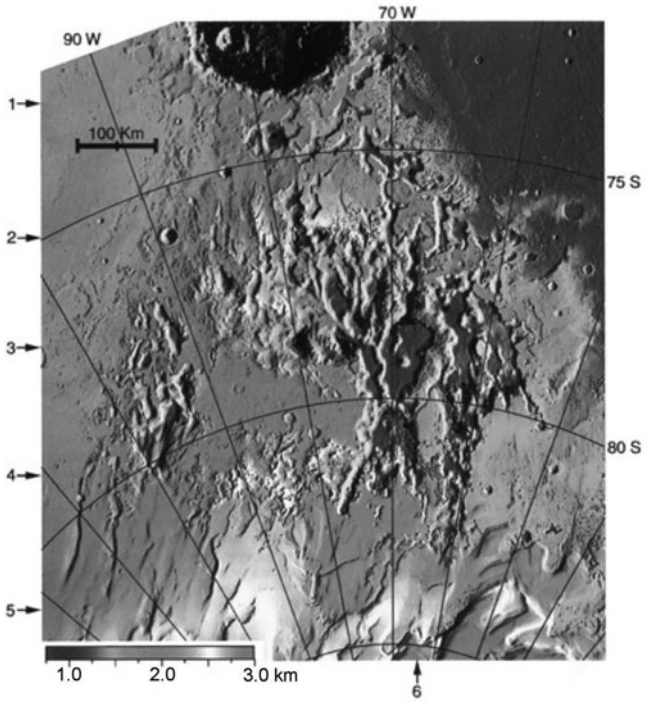


Fig. 16. Altimetric map showing the location and characteristics of the multiple deep depressions forming Cavi Angusti and their relationship to the smooth region to the northeast thought to represent a contemporaneous lake environment (Head and Pratt, 2001).

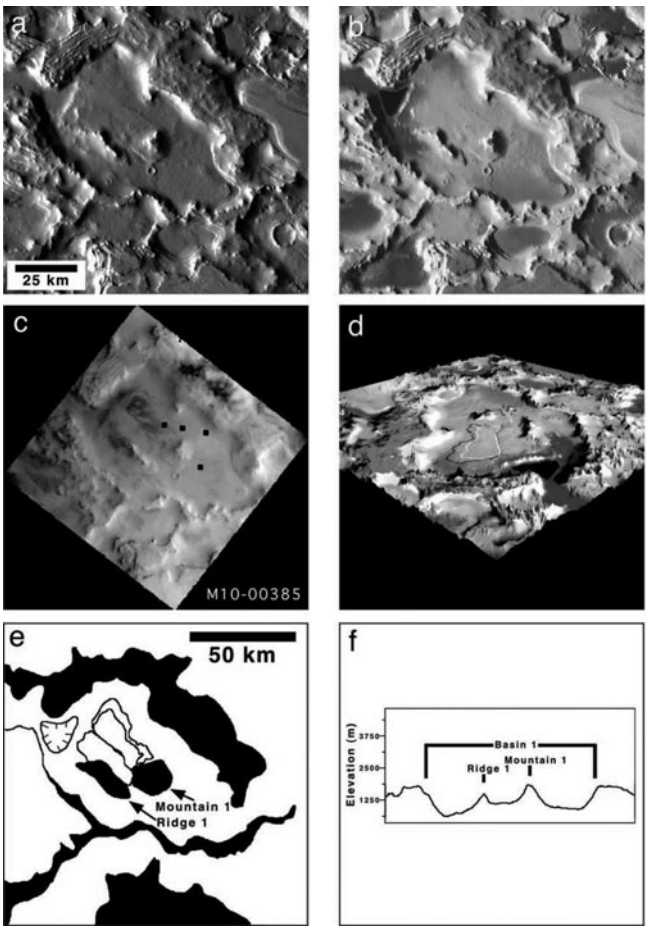


Fig. 17. Details of the largest depression in Cavi Angusti (location is CA in Fig. 20) and the ridges and lobate features thought to represent subglacial eruptions leading to melting and the formation of the large depression. (a) Shaded relief. (b) MOLA topography. (c) MOC wide-angle image. (d) Perspective view. (e) Sketch map showing mountains, ridge and flow-like lobes thought to be of subglacial volcanic origin. (f) MOLA altimetric profile across the short axis of the basin showing the mountain and ridge (Ghatan and others, 2003).

and extending further downslope (e.g. Shean and others, 2005). Additional scarps within the Pavonis deposits, as well as broad depressions and scarps within the Ascreaus Mons fan-shaped deposit (e.g. Parsons and Head, 2004), are evidence that ice-marginal volcanic interaction was an important process on Mars, and that in the case of the tropical mountain glaciers (e.g. Head and Marchant, 2003), extended over a significant period of time.

An additional example of synglacial volcanism is related to the abundant lava flows cascading over the Olympus Mons scarp in the vicinity of the numerous debris-covered piedmont glaciers (e.g. Lucchitta, 1981; Basilevsky and others, 2005; Milkovich and others, 2006). There, clear evidence exists for the development of numerous extensive piedmont glaciers and the subsequent descent of lava flows over these deposits, both when ice remained in the deposits and subsequent to its loss.

Postglacial volcanism and interaction with snow and ice deposits

Subsequent to periods of active glaciation, volcanic activity can interact with the remaining glacial deposits. In the case

https://doi.org/10.3189/172756407782282570 Published online by Cambridge University Press

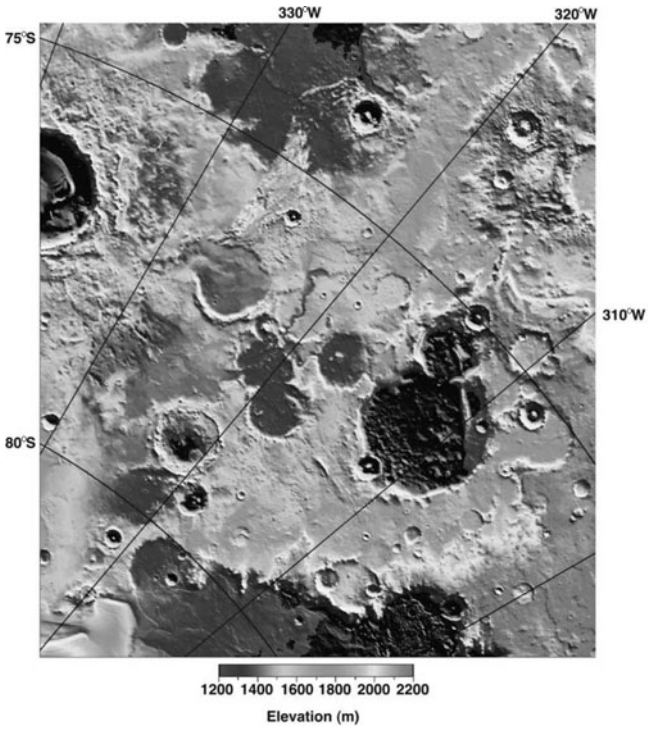


Fig. 18. Meltwater channels emerging from the eastern edge of the Dorsa Argentea Formation. MOLA altimetric map of the deposit (top) and the channels and ponds (middle, lower); features labeled in Figure 19.

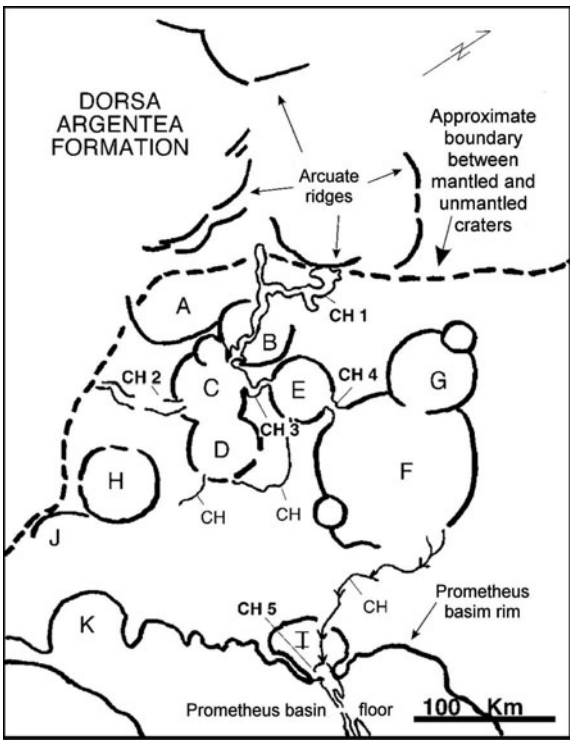


Fig. 19. Meltwater channels emerging from the eastern edge of the Dorsa Argentea Formation. Sketch map showing the main features and meltwater pathways (channels). See Figure 13 for location. Letters refer to different craters and CH to different channels described in Milkovich and others (2002).

of Arsia Mons, lava flows from the upper flanks of Arsia embay and invade the tropical mountain glacier deposit (e.g. Scott and Zimbelman, 1995). Recent high-resolution data reveal the intrusion of a dike and formation of tephra cones and flows above the dike within the ridged facies (drop moraines) of the glacial deposit (Fig. 21). Although direct evidence of heating and melting of ice has not yet been found, it is clear that the detailed structure and texture of the glacial deposits have controlled the direction of lava flow. Flows follow parallel drop moraines and migrate between low points in the moraines. The large terminal moraine of the deposit has been breached, and the flow has extended out of the glacial deposit into the surrounding lava plains (Fig. 21). Although this large terminal ridge could conceivably have been ice-cored, as yet no evidence exists for liquid meltwater having been generated in the vicinity of the breach as a result of the proximity of the lavas. Nonetheless, these types of relationships should be examined for evidence that post-glacial volcanism might have generated meltwater, thereby revealing the presence of remnant ancient ice deposits.

CONCLUSION

The basic principles of heat transfer and melting in subglacial volcanic eruptions and implications for volcanic deposit morphology and meltwater volumes (e.g. Wilson and Head, 2002) provide a basis for the identification and interpretation of the general environments and geological settings of magma–water interactions on Mars (e.g. Head and Wilson, 2002). We have highlighted advances in the last five years in the understanding of the distribution of ice on the surface of Mars and in the Martian cryosphere and

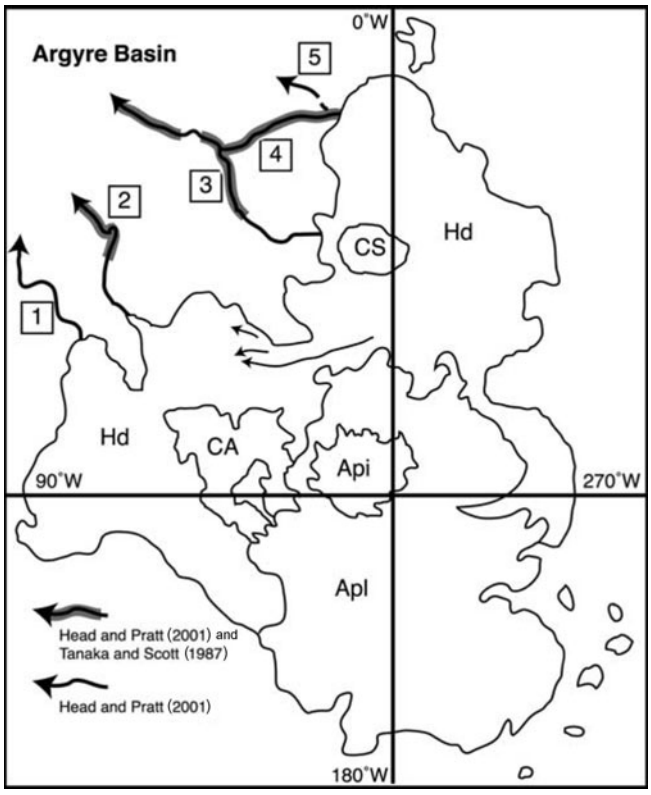


Fig. 20. Channels emanating from the western side of the Dorsa Argentea Formation (Hd) and flowing down into the Argyre basin. Also shown are the traces of the channels back into the ice-sheet deposit. CA (Cavi Angusti); CS (Cavi Sisyphi) (Ghatan and Head, 2004). Api (Amazonian polar ice deposit); Apl (Amazonian polar layered deposit). Compare to Figure 13 for location and context.

https://doi.org/10.3189/172756407782282570 Published online by Cambridge University Press

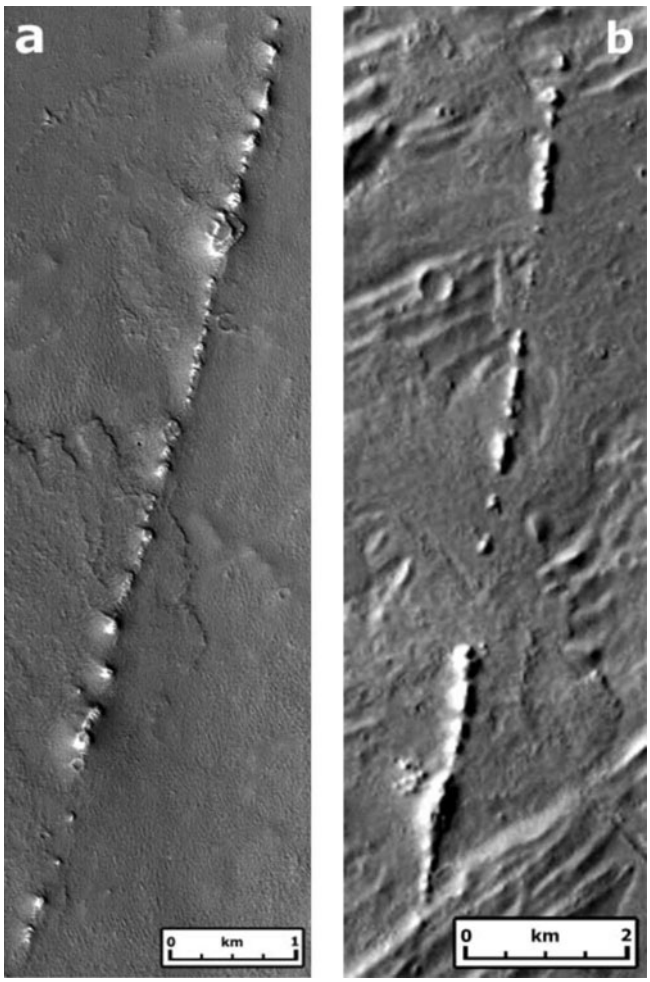


Fig. 21. Post-glacial volcanism in the ridged deposit of Arsia Mons. Rows of volcanic cones and adjacent flows superimposed on the Arsia Mons fan-shaped tropical mountain glacier deposit. (a) Southern segment showing cones and adjacent flows. (b) Northern segment showing cones and the interaction of adjacent flows with ridges interpreted to be glacial drop moraines that could have contained ice cores at the time of eruption (Head and others, 2005a).

described new insights into the importance of volcano–ice interactions, applying our understanding of basic heat transfer mechanisms. We conclude that volcano–ice interactions, by way of emplacement of dikes and sills, were critical for penetrating cryospheric seals to release the groundwater that created the outflow channels. Morphologic evidence for dike emplacement, phreatomagmatic eruptions and sill-induced melting and collapse provide guidelines for recognition of additional occurrences. Recognition of tropical mountain glacier deposits has led to improved criteria for the recognition on Mars of subglacial dike and sill emplacement, subglacial flows, glacier margin and supraglacial volcanic deposits, as well as possible jökulhlaup channels and deposits. Finally, the examination of the Dorsa Argentea Formation circumpolar ice sheet has revealed multiple examples of subglacial volcanoes and recognition of the meltwater pathways (interior channels, pits, depressions, eskers, marginal ponds, lakes and channels) largely related to syneruption melting. These examples will serve to enhance the detection, documentation, modeling and understanding of volcano–water interactions on Mars.

ACKNOWLEDGEMENTS

We gratefully acknowledge financial support from the NASA Mars Data Analysis Program (MDAP) (Grant NNG04 GJ99G) and the NASA Planetary Geology and Geophysics Program (Grant NNG05 G121G). Thanks are extended to J. Dickson and A. Côté for help with the preparation of the manuscript and to B. Edwards and S. Lane for helpful reviews.

REFERENCES

Baker, V.R. 2001. Water and the Martian landscape. *Nature,* **412**, 228–236.

Basilevsky, A.T. *and 10 others*. 2005. Morphology and geological structure of the western part of the Olympus Mons volcano on Mars from the analysis of the Mars Express HRSC imagery. *Solar System Res.,* **39**(2), 85–101.

Björnsson, H. 1992. Jökulhlaups in Iceland: prediction, characteristics and simulation. *Ann. Glaciol.,* **16**, 95–106.

Carr, M.H. 1996. *Water on Mars*. New York, NY, Oxford University Press.

Chapman, M.G. 1994. Evidence, age and thickness of a frozen paleolake in Utopia Planitia, Mars. *Icarus,* **109**, 393–406.

Chapman, M.G. *and 7 others*. 2000. 'Fire and ice': volcanism and ice interactions on Earth and Mars. *In* Zimbelman, J.R. and T.K.P. Gregg, *eds. Environmental effects on volcanic eruptions: from deep oceans to deep space*. New York, NY, Kluwer Publishing, 39–73.

Clifford, S.M. 1993. A model for the hydrologic and climatic behaviour of water on Mars. *J. Geophys. Res.,* **98**, 10,973–11,016.

Dickson, J.L. and J.W. Head. 2006. Evidence for an Hesperian-aged south circum-polar lake margin environment on Mars. *Planet. Space Sci.,* 54, 251–272.

Fastook, J.L., J.W. Head, D.R. Marchant and D.E. Shean. 2005. Ice sheet modelling: mass balance relationships for map-plane ice sheet reconstruction: application to Tharsis Montes glaciation. *In Lunar and Planetary Science Conference XXXVI*. CD Rom.

Forget, F., R.M. Haberle, F. Montmessin, B. Levrard and J.W. Head. 2006. Formation of glaciers on Mars by atmospheric precipitation at high obliquity. *Science,* **311**(5759), 368–371.

Ghatan, G.J. and J.W. Head, III. 2002. Candidate subglacial volcanoes in the south polar region of Mars: morphology, morphometry, and eruption conditions. *J. Geophys. Res.,* **107**(E7), 5048. (10.1029/2001JE001519.)

Ghatan, G.J. and J.W. Head, III. 2004. Regional drainage of meltwater beneath a Hesperian-aged south circumpolar ice sheet on Mars. *J. Geophys. Res.,* **109**, E07006. (10.1029/2003JE002196.)

Ghatan, G.J., J.W. Head, III and S. Pratt. 2003. Cavi Angusti, Mars: characterization and assessment of possible formation mechanisms. *J. Geophys. Res.,* **108**(E5), 5045. (10.1029/2002JE001972.)

Ghatan, G.J., J.W. Head and L. Wilson. 2005. Mangala Valles, Mars: assessment of early stages of flooding and downstream flood evolution. *Earth, Moon Planets,* **96**(1–2), 1–57.

Guðmundsson, M.T., F. Sigmundsson and H. Björnsson. 1997. Ice-volcano interaction of the 1996 Gjálp subglacial eruption, Vatnajökull, Iceland. *Nature,* **389**(6654), 954–957.

Head, J.W. 2006. The hydrological cycle on Mars: The transition from a vertically integrated to a horizontally integrated system. *In Brown Vernadsky Microsymposium 44*. CD Rom.

Head, J.W. and B. Hallet. 2001. Origin of sinuous ridges in the Dorsa Argentea formation: new observations and tests of the esker hypothesis. *In Lunar and Planetary Science Conference XXXIII*.

Head, J.W., III and S. Pratt. 2001. Extensive Hesperian-aged south polar ice sheet on Mars: evidence for massive melting and retreat, and lateral flow and ponding of meltwater. *J. Geophys. Res.,* **106**(E6), 12,275–12,300.

https://doi.org/10.3189/172756407782282570 Published online by Cambridge University Press

Head, J.W. and L. Wilson. 2002. Mars: a review and synthesis of general environments and geological settings of magma H20 interactions. *In* Smellie, J. L. and M.G. Chapman, *eds. Volcano–ice interaction on Earth and Mars*. London, Geological Society, 27–58. (Special publications 202.)

Head, J.W. and D.R. Marchant. 2003. Cold-based mountain glaciers on Mars: Western Arsia Mons. *Geology,* **31**(7), 641–644.

Head, J.W., J.F. Mustard, M. Kreslavsky, R.E. Milliken and D.R. Marchant. 2003a. Recent ice ages on Mars. *Nature,* **426**(6968), 797–802.

Head, J.W., L. Wilson and K.L. Mitchell. 2003b. Generation of recent massive water floods at Cerberus Fossae, Mars by dike emplacement, cryospheric cracking, and confined aquifer groundwater release. *Geophys. Res. Lett.,* **30**(11). (10.1029/2003GL017135.)

Head, J.W., III, D.R. Marchant and G.J. Ghatan. 2004. Glacial deposits on the rim of a Hesperian-Amazonian outflow channel source trough: Mangala Valles, Mars. *Geophys. Res. Lett.,* **31**, L10701. (10.1029/2004GL020294.)

Head, J.W., D.E. Shean and L. Wilson. 2005a. Post-glacial dike emplacement event at Arsia Mons, Mars: eruptive spatter cones, tephra cones and flows along a dike-related fissure. *In Brown Vernadsky Microsymposium 42*. CD Rom.

Head, J.W. *and 12 others*. 2005b. Tropical to mid-latitude snow and ice accumulation, flow and glaciation on Mars. *Nature,* **434**(7031), 346–351.

Head, J.W., D.R. Marchant, M.C. Agnew, C.I. Fassett and M.A. Kreslavsky. 2006a. Extensive valley glacier deposits in the northern mid-latitudes of Mars: evidence for Late Amazonian obliquity-driven climate change. *Earth Planet Sci. Lett.,* **241**(3–4), 663–671.

Head, J.W., L. Wilson, J. Dickson and G. Neukum. 2006b. The Huygens-Hellas giant dike system on Mars: implications for Late Noachian-Early Hesperian volcanic resurfacing and climatic evolution. *Geology,* **34**(4), 285–288.

Head, J.W., A.L. Nahm, D.R. Marchant and G. Neukum. 2006c. Modification of the dichotomy boundary on Mars by Amazonian mid-latitude regional glaciation. *Geophys. Res. Lett.,* **33**, L08S03. (10.1029/2005GL024360.)

Howard, A. D. 1981. Etched plains and braided ridges of the south polar region of Mars: features produced by basal melting of ground ice? NASA Technical Memorandum, NASA-TM-84211. 286–289. Washington, DC.

Leask, H.J., L. Wilson and K.L. Mitchell. 2006a. Formation of Aromatum Chaos, Mars: morphological development as a result of volcano–ice interactions. *J. Geophys. Res.,* **111**, E08071. (10.1029/2005JE002549.)

Leask, H.J., L. Wilson and K.L. Mitchell. 2006b. Formation of Ravi Vallis outflow channel, Mars: morphological development, water discharge, and duration estimates. *J. Geophys. Res.,* **111**, E8070. (10.1029/2005JE002550.)

Lucchitta, B.K. 1981. Mars and Earth: comparison of cold-climate features. *Icarus,* **45**(2), 264–303.

Marchant, D.R. and J.W. Head. 2003. Cold-based glaciers in the western Dry Valleys of Antarctica: terrestrial landforms and Martian analogues. In Lunar and Planetary Science XXXIV: papers presented to the 34th lunar and plantetary science conference. CD Rom.

Milkovich, S.M., J.W. Head, III and S. Pratt. 2002. Meltback of Hesperian-aged ice-rich deposits near the south pole of Mars: evidence for drainage channels and lakes. *J. Geophys. Res.,* **107**(E6). (10.1029/2001JE001802.)

Milkovich, S.M., J.W. Head and D.R. Marchant. 2006. Debris-covered piedmont glaciers along the northwest flank of the Olympus Mons scarp: evidence for low-latitude ice accumulation during the Late Amazonian of Mars. *Icarus,* **181**(2), 388–407.

Neukum, G. *and 10 others*. 2004. Recent and episodic volcanic and glacial activity on Mars revealed by the High Resolution Stereo Camera. *Nature,* **432**(7020), 971–979.

Parsons, R.L. and J.W. Head. 2004. Ascraeus Mons, Mars: characterisation and interpretation of the fan-shaped deposit on its western flank. *In Lunar and Planetary Science Conference XXXV*. CD Rom.

Russell, P.S. and J.W. Head. 2003. Elysium-Utopia flows as megalahars: a model of dike intrusion, cryosphere cracking, and water-sediment release. *J. Geophys. Res.,* **108**(E6), 5064. (10.1029/2002JE001995.)

Scott, D.H. and J.R. Zimbelman 1995. Geologic map of Arsia Mons Volcano, Mars. Map no. 1–2480. USGS Misc. Invest. Ser. US Geological Survey.

Shean, D.E., J.W. Head and D.R. Marchant. 2005. Origin and evolution of a cold-based tropical mountain glacier on Mars: the Pavonis Mons fan-shaped deposit. *J. Geophys. Res.,* **110**, E05001. (10.1029/2004JE002360.)

Tanaka, K.L. and D.H. Scott 1987. Geologic map of the polar regions of Mars. Map no. I-1802-C. USGS Misc. Invest. Ser. US Geological Survey.

Tanaka, K.L. and E.J. Kolb. 2001. Geologic history of the polar regions of Mars based on Mars Global Surveyor data: I. Noachian and Hesperian periods. *Icarus,* **154**(1), 3–21.

Wilson, L. and J.W. Head. 2002. Heat transfer and melting in subglacial basaltic volcanic eruptions: implications for volcanic deposit morphology and meltwater volumes. *In* Smellie, J. L. and M.G. Chapman, *eds. Volcano-ice interaction on Earth and Mars*. London, Geological Society, 5–26. (Special publications 202.)

Wilson, L. and P.J. Mouginis-Mark. 2003. Phreatomagmatic explosive origin of Hrad Vallis, Mars. *J. Geophys. Res.,* **108**(E8), 5082. (10.1029/2002JE001927.)

Wilson, L. and J.W. Head, III. 2004. Evidence for a massive phreatomagmatic eruption in the initial stages of formation of the Mangala Valles outflow channel, Mars. *Geophys. Res. Lett.,* **31**, L15701. (10.1029/2004GL020322.)

Wilson, L. and J.W. Head, III. 2007. Heat transfer in volcano–ice interactions: synthesis and applications to processes and landforms on Earth. *Ann. Glaciol.,* **45**, 83–86.

Wilson, L., D.E. Shean and J.W. Head, III. 2005. Subglacial dike emplacement on Mars: radial ridges associated with the Pavonis Mons fan-shaped deposit. *In Lunar and Planetary Science Conference, XXXVI*. CD Rom.

https://doi.org/10.3189/172756407782282570 Published online by Cambridge University Press